Chapter 13
Magnetic Nanoparticles for Life Sciences Applications

C. Marquina

Abstract The ongoing research on the applications of magnetic nanoparticles in Bio-medicine and the results obtained up to now open a wide range of possibilities for their use in Life Science disciplines, for example in general plant research and agronomy. The work presented here focuses on the interaction of two types of magnetic core-shell nanoparticles with plants and microorganisms. The research carried out with carbon coated iron nanoparticles aims to investigate their penetration and translocation in whole living plants and into plant cells, as response of the nanoparticles to magnetic field gradients. This study is essential to evaluate the suitability of any nanoparticles as magnetic responsive carriers for the localized delivery of phytosanitary or pest control treatments. The study carried out with silica coated nanoparticles focuses on their interaction with fungal cells, taking a soil borne plant pathogen as in vitro model. Our research paves the way to use magnetic nanoparticles for detection, selective control and eventual elimination of pathogenic fungi.

13.1 Introduction

Life Sciences encompass the study of living organisms, which concerns not only animals (including human beings) but also plants and microorganisms, covering fields of knowledge such as Medicine, Biotechnology, Environmental Sciences, Botany and other branches of Biology, among many others. Research on these subjects has acquired a marked interdisciplinary character which has made it benefit, for example, from the knowledge, materials, devices and tools of Nanoscience and Nanotechnology. An example is the increasingly frequent use of nanoparticles, and in particular, of magnetic nanoparticles, in Biomedicine. Here we will focus on the use

C. Marquina (✉)
Instituto de Nanociencia y Materiales de Aragón (INMA), Consejo Superior de Investigaciones Científicas (CSIC)-Universidad de Zaragoza, Pedro Cerbuna 12, 50009 Zaragoza, Spain
e-mail: clara@unizar.es

Departamento de Física de la Materia Condensada, Facultad de Ciencias, Universidad de Zaragoza, Pedro Cerbuna 12, 50009 Zaragoza, Spain

D. Peddis et al. (eds.), *New Trends in Nanoparticle Magnetism*,
Springer Series in Materials Science 308,
https://doi.org/10.1007/978-3-030-60473-8_13

of magnetic nanoparticles in Life Sciences fields dealing with plants and microorganisms. Although Nanoscience and Nanotechnology are more and more present in areas such as plant research, agriculture and agronomy, and the incorporation to these areas of new strategies and methodologies based on the use of nanoparticles is growing, the particular case of magnetic nanoparticles is still little explored.

One of the first works dealing with nanoparticles in plant research is the one carried out by Torney et al. [1] in which mesoporous silica nanoparticles act as vehicles to transport DNA and chemicals into isolated plant cells and intact leaves. The delivery of DNA by means of mesoporous SiO_2 nanoparticles was studied also by Martín-Ortigosa et al. making use of different strategies for the penetration of the nanoparticles into the plant cell [2–4]. Polymeric nanoparticles [5], fluorescent chromophores [6], ZnO nanoparticles [7], among many others have also been used as carriers for plant cell genetic engineering, one of the most studied applications in plant research. Another topic that has aroused great interest is the study of how nanoparticles can influence the plant growth and germination and the functionality of plant cell organelles. Hong et al. studied effect of TiO_2 nanoparticles on the photochemical reaction of chloroplast of *Spinacia oleracea* [8], and on the growth of spinach plants [9]. Recently, Frazier et al. studied the influence of these nanoparticles on the growth and microRNA expression of tobacco (*Nicotiana tabacum*) [10]. The effect of ZnO nanoparticles on the inhibition of seed germination and root growth was also studied by Lin and coworkers [11, 12]. Efforts have also been focused on enhancing crop yields and controlling/suppressing plant diseases and parasites. With these objectives in mind, studies have been carried out with a variety of nanoparticles (made of polymers, liposomes, 3d-metals and 3d-metal oxides, carbon nanostructures etc.) as reported for example in the works of Perez de Luque et al. [13], Servin and coworkers [14] and Yasmeen et al. [15]. For the control of diseases and pests, the rapid and easy detection of the causative agent is crucial. In this respect, Nanotechnology has provided us with highly sensitive, versatile, inexpensive and user-friendly biosensors [16–19]. Among the different types, nano-devices based on the localized surface plasmon resonance (LSPR) have been developed, for example, for the detection of the maize chlorotic mottle virus in infected maize seeds [20, 21]; or for detecting biomarkers associated with nutritional deficiencies in crops [22]; or to elucidate the effect of a T-DNA insertion on mRNA transcripts in plants [23, 24], among other applications. With regard to microorganisms, the use of micro- and nano-particles as an antibacterial and antifungal agent is widespread. Silver is one of the most frequently used materials [25], working for example against phytopathogenic fungi [26] and bacteria such as *Pseudomonas aeruginosa* and *Staphylococcus aureus* [27]. Recent studies carried out on plant pathogenic fungi, oomycete and bacteria, have shown that copper nanoparticles can enhance the effect of commercial antimicrobial copper formulations and even represent an efficient alternative [28]. Zinc oxide and magnesium oxide nanoparticles have also demonstrated their effectiveness as antimicrobials [29–33].

The significant progress made in Biomedicine derived from the use of magnetic nanoparticles in diagnostic and therapy has opened the doors to their implementation

in the applications just mentioned. In addition, the capability of magnetic nanoparticles to interact with a magnetic field increases the possibilities for their exploitation. For instance, in the same way as nanoparticles can act as vehicles for magnetically targeted drug delivery in chemotherapy against cancer [34, 35] they could be implemented in phytosanitary treatments, for the selective and controlled delivery of agrochemicals or other biomolecules, or to induce genetic transformations etc. [13]. Also in the analogy with biomedical applications, magnetic nanoparticles could play a role as MRI contrast agents for plant research. In fact this technique is as well suitable for studying the health of a plant in a non-destructive way [36], and has made possible the study of the modifications of the biophysical parameters of a cucumber plant as response to environmental changes [37], the changes in the dynamics of the sap flow [38], or the damage induced by plant parasitic nematodes and soil borne pathogens on sugar beet plants [39]. Even the localized heating by magnetic hyperthermia [40] might be as well a useful treatment in agriculture and agronomy. As suggested by Pérez de Luque and Rubiales [13], it might be applied to eliminate parasitic weeds, assuming that nanoparticles are able to accumulate in a specific plant organ. This could be the case, for example, of tubercles in *Orobanche crenata*, where the nanoparticles (administered for example by the roots) would accumulate due to their sink effect.

As is well known, magnetic nanoparticles can be coated with biocompatible materials as silica [41, 42], dextran [43], polyvinyl alcohol (PVA) [44], poly(ethylene glycol) (PEG) [45] etc., which allows modifying the particle surface with a large number of molecules of biological interest, and therefore broadening the functionality of the nanoparticle. The coating can be functionalized with bio-molecules, as for instance antibodies [46, 47], able to recognize a specific pathogen in a culture or soil, making the nanoparticle act as a magnetic label for the pathogen to be detected by a biosensor [17, 18, 48]. The diversity of materials that can be used as coating and the wide variety of functionalization protocols make the magnetic nanoparticles very promising tools for plant biology and biotechnology.

In the following sections we will deal with two types of core-shell magnetic nanoparticles. In the first case, they consist of an iron core coated with graphite/graphene layers; from here on they will be called carbon-coated (Fe@C) nanoparticles. The second type is magnetite coated with silica (i.e., $Fe_3O_4@SiO_2$) nanoparticles; this coating, besides being biocompatible, stable and suitable for the encapsulation of biomolecules, [49] is very easy to be functionalized with biological moieties [46]. Likewise, the biocompatibility of the Fe@C nanoparticles has been successfully tested in in vitro and in vivo animal models [35, 50, 51]. In particular, the experiments carried out in New Zeeland rabbits have shown that these nanoparticles, once injected into the animal, can be located in the desired organ or tissue with the aid of a magnetic field gradient created by an implanted magnet. In addition, it has been shown that the nanoparticle coating can adsorb and desorb a chemotherapeutic agent, so they can be used for magnetically driven drug delivery [35]. These experiments suggest that nanoparticles could also be utilized *in planta*, as magnetic carriers of phytosanitary agents, nutrients, enzymes, nucleic

acids etc. to be concentrated in a specific part or organ of a plant (e.g., where a parasite or infection is located, or where the nutrients are going to be adsorbed in a more effective manner, etc. [52]). An advantage of using the Fe@C and the Fe_3O_4@SiO_2 nanoparticles in these applications is the high specific surface area of the coating, which offers a high load capacity [49, 53]. This could help in the optimization of the dose to be delivered, without the need of repeating the treatment, which would lead to more efficient and sustainable agricultural practices and methods.

In any case, taking these ideas to practice requires, among other issues, the study of the nanoparticle response when a magnetic field gradient is applied to the plant, and the analysis of their transport and distribution *in planta.* The experiments conducted for this purpose are presented in the following sections. They were carried out with Fe@C nanoparticles and different type of crops [52, 54, 55], constituting a pioneering work regarding the use of magnetic nanoparticles in whole alive plants. Next section also reports what, to our knowledge, is the first study on the interaction between magnetic nanoparticles and fungal cells. The final objective was to evaluate the feasibility of new nanotechnology-based strategies for the early detection and control of pathogenic fungi in plants, crops and soils [48]. The final goal was the design of a biosensor combining immunological recognition and magnetic detection [17, 18]. In this case, the study was performed with Fe_3O_4@SiO_2 nanoparticles, given the possibility to functionalize the coating with an antibody that recognized the pathogenic fungus. The target is *Fusarium oxysporum*, a soil borne plant pathogen that infects a vast variety of crops and is the cause of important economic losses [56]. It is also an opportunistic human pathogen and infection can also result in the death of immunocompromised patients [57]. To date there are neither effective methods for an early detection of the fungus, nor treatments for a complete elimination. In the case of *F. oxysporum* the problem is even more complex, because pathogenic strains cohabit in the rhizosphere with nonpathogenic strains, leading to biological control [58]. Therefore, in the present case an adequate functionalization strategy that ensures the high selectivity and sensitivity in the detection prior to the treatment is crucial. In addition, a comprehensive study of the behavior of the fungus in the presence of the nanoparticles, as the one reported here, and a deep knowledge of the toxicity profile of these nanomaterials are also decisive.

13.2 Penetration and Transport of Magnetic Nanoparticles in Living Plants

The aim of this work was to visualize the transport of nanoparticles inside living plants, and also to investigate whether the nanoparticles respond to the application of magnetic field gradients, with the objective of concentrating them in localized areas of the plants by the use of small magnets. As mentioned before, the work described from here on was carried out with whole living plants.

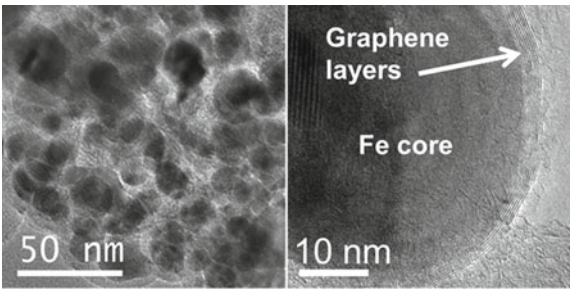

Fig. 13.1 High Resolution-TEM images of Fe@C nanoparticles (left) and magnification showing the graphene layers coating the Fe core (right)

The Fe@C nanoparticles were synthesized in an arc-discharge furnace [50, 59–61] by a method based on the previously followed by Krätschmer and coworkers [62]. The nanoparticles are produced by the sublimation and subsequent condensation of the starting materials (iron micrometric powder inside a graphite rod) when the electric arc ionizes the helium gas in the furnace chamber. The sublimation of graphite and iron produces a soot that, when condensed, deposits on the chamber walls. This soot was analyzed by X-ray diffraction (XRD). According to the XRD spectrum this powder contains mainly α-Fe, and some small traces of magnetite/maghemite. A more detailed characterization was carried out by Transmission Electron Microscopy (TEM) [50, 59, 61]. TEM images showed that the obtained black powder contained a variety of carbon nanostructures, including carbon onions, some nanotubes, amorphous carbon and a large proportion of iron/iron oxide nanoparticles encapsulated in graphene/graphite layers, as the ones displayed in Fig. 13.1.

The size of the nanoparticles ranged between 5 and 50 nm, with the size distribution center at 10 nm. The TEM images showed as well that the soot contained a small amount of non-coated or partially coated metallic particles. These are not biocompatible and therefore had to be eliminated from the sample by chemical etching [35, 61]. To increase the concentration of magnetic nanoparticles in the final sample, a magnetic purification of the powder was carried out to eliminate the amorphous carbon and all those carbon structures not containing any magnetic nanoparticle. For this purpose, particles were suspended in distilled water and the separation was carried out by placing the suspension in a magnetic field gradient produced by 3kOe permanent magnet [35]. After drying the fraction containing the magnetic nanoparticles these were suspended in two different biocompatible fluids, keeping the suspension in an ultrasonic bath for several minutes. A suspension was prepared with gelafundin, as this a biocompatible commercial succinated gel had been already tested in the above mentioned in vivo experiments with New Zeeland rabbits [35] and mice [51]. The other suspension was prepared with mannitol, a solution commonly used in experiments with plants [63]. These biocompatible magnetic fluids were subsequently administered to the plants, which represents an alternative to other methods used when working with plants [2, 3, 64]. To study the possible differences in the translocation and accumulation of the nanoparticles inside the plant, three different administration methods were tested: by injection, by spraying and by immersing the plant roots directly into the nanoparticle solution.

13.2.1 Nanoparticle Application by Injection

These experiments were carried out on living pumpkin plants and with the Fe@C nanoparticles suspended in gelafundine. The pumpkin plants were selected because of the large size of their vessels, to make the transport of the nanoparticles through the vascular system easier. Plants were grown as described in [52, 54, 63]. In a first series of experiments, the biocompatible magnetic fluid was injected inside the internal cavity of a leaf petiole (see Fig. 13.2 left), on the assumption that it would penetrate into the plant and translocate to other areas through the vascular tissues. To check if after injection it was possible to concentrate the nanoparticles in certain regions of the plant, permanent magnets (in the form of small discs about 5 mm diameter) were placed on the leaf petiole opposite to the injection point and on the roots, as shown in Fig. 13.2 left [52, 54]. On the right, the figure shows as well an optical micrograph of the transverse section of a pumpkin stem, with the main structural elements.

Plant tissue samples were collected 24, 48, 72 and 168 h after the injection of the magnetic fluid and processed for microscopy analysis. Tissue was cut from the stem and leaf petiole at the injection point. Roots and petiole samples were collected at the point of magnets localization but also before and after the magnet position (i.e., facing the expected movement of the nanoparticles from the injection point through the vascular tissue towards the magnet). The collected samples were observed using light microscopy, under a confocal laser scanning microscope and by TEM. Details on sample processing and observing protocols for the respective methods can be found in [52, 54].

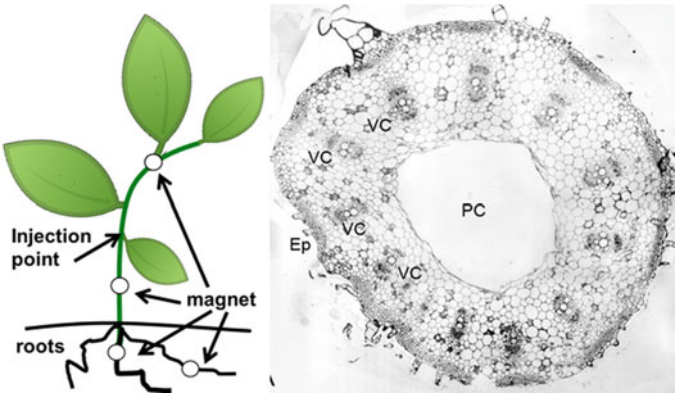

Fig. 13.2 Scheme showing the nanoparticle suspension injection point and the magnet positions (left). Optical micrograph of a pumpkin stem transversal section (right); VC stands for the vascular core, Ep for the epidermis and PC for the pit cavity. Reprinted by permission from Springer Nature Customer Service Centre GmbH: Springer Nature BMC Plant Biology Nanoparticle Penetration and transport in living pumpkin plants: in situ subcellular identification, Corredor et al. [54]. Copyright © 2009. https://doi.org/10.1186/1471-2229-9-45

To assess whether the nanoparticles would penetrate into the living plant and travel through the vascular system to the places where the magnets were located hand-cut sections of petioles and roots were observed on a light microscope. Figure 13.3 shows the images corresponding to sections of petioles (upper row) and of roots (lower row), taken at the injection point (a), before the position of the magnet (d), at the magnet point (b and e) and after the magnet position (c and f). The dark colored areas correspond to the accumulation of the nanoparticles suspension. Figure 13.3a shows a detail of the vascular tissue (vc in Fig. 13.2 right) at the application point where nanoparticles penetrated. They further moved to other parts of the plant and the magnets concentrated the fluid in the vascular tissues adjacent to their localization in the petiole (Fig. 13.3b) and roots (Fig. 13.3d, e). By comparison, images taken in vascular areas opposite to the magnet point of the same sections (Fig. 13.3c) or in samples located after the magnet position (Fig. 13.3f) display almost no black color, indicating that the nanoparticles in the fluid are trapped by the magnet and they do not travel further.

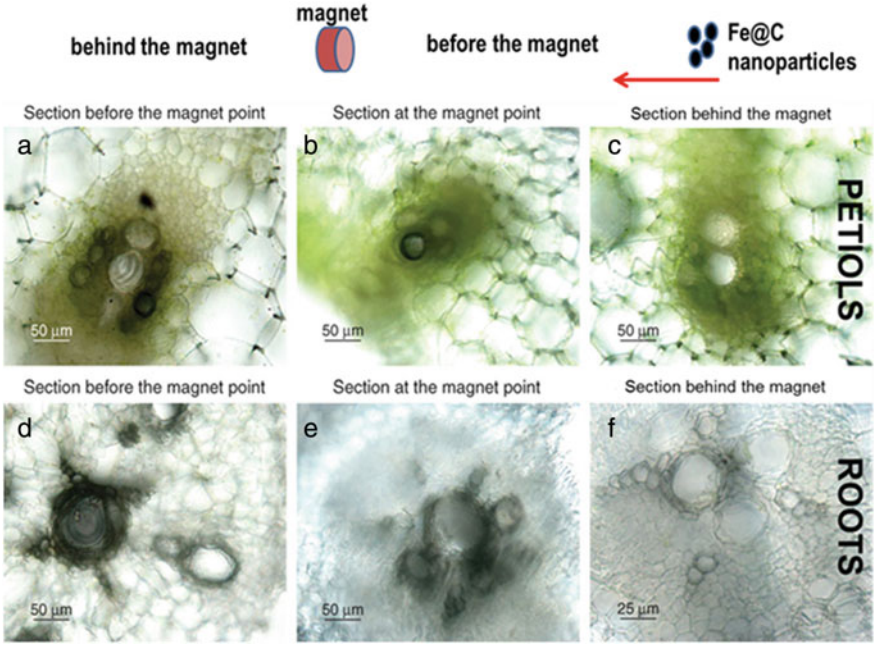

Fig. 13.3 Light microscopy images of vascular tissue of the petiole cut **a** at the application point; **b** adjacent to a magnet; **c** opposite to a magnet. Light microscopy images of vascular tissue of the root tissue cut **d** before the position of the magnet; **e** at the position of the magnet; **f** behind the magnet. Printed by permission from Oxford University Press Annals of Botany Nanoparticles as Smart Treatment-delivery Systems in Plants: assessment of different techniques of Microscopy for their Visualization in Plant Tissues, González-Melendi et al. [52]. Copyright © 2007 https://doi.org/10.1093/aob/mcm283

Tissue sections were also imaged by confocal and fluorescence microscopies. Despite the fact that the size of the nanoparticles is below the resolution limit of the light microscope, nanoparticle aggregates were clearly visualized by the differential interference contrast (DIC) or Nomarski technique on a projection of a 3D confocal stacks, and also in reflection mode. Figure 13.4a shows nanoparticles inside a cell of the cortex next to the internal hollow of the petiole just before the position of the magnet, 72 h after the injection. The image corresponds to the overlay of the respective images taken in Nomarski and reflection modes. On the contrary, no particles were observed in images from the untreated plant used as controls. Nanoparticles were also detected in the cell wall of the xylem vessel cells. This cell wall is naturally auto-fluorescent due to the lignin as its major component. Due to their black color (because their graphitic shell) the Fe@C nanoparticles are very suitable for working with plant tissues, as they can be easily identified in bright field images (as the one in Fig. 13.4b), and also be seen as non-auto-fluorescent dots in the cell wall, like in Fig. 13.4c.

Some samples were studied by light microscopy, and then the same regions were analyzed by TEM. Unlike in the control samples, aggregates of nanoparticles were detected at the injection site 24 h after administration, in the epidermis and in the extracellular space in between cells of the epidermal layer, on a light microscope under phase contrast (Fig. 13.5a). Electron microscopy correlative analysis displayed several nanoparticle aggregates (marked by asterisks in Fig. 13.5b) that would correspond to those previously detected by light microscopy. Increasing the magnification, individual nanoparticles could be clearly visualized (Fig. 13.5c), to measure their size. The diameter of the biggest particles is around 50 nm, although they represent the

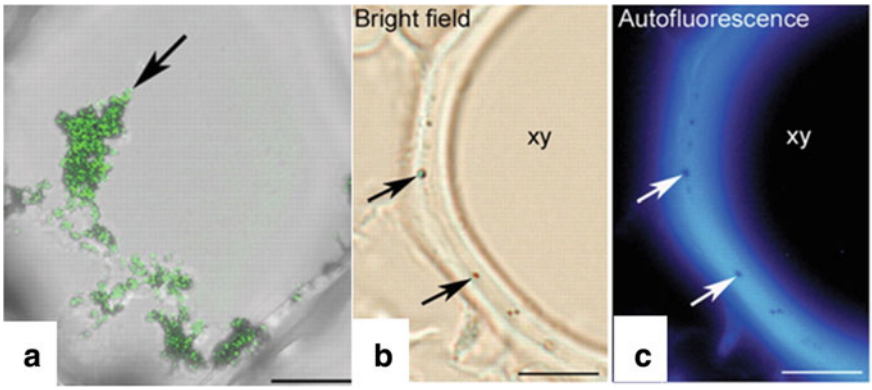

Fig. 13.4 Nanoparticles (pointed by arrows) in a projection of 3-D confocal stacks of a cell of a plant stem at the position of the magnet, 72 h after the suspension injection **a**. Nanoparticles (pointed by arrows) in a confocal bright-field image **b** and in a fluorescence microscope image **c** of a section of plant tissue. Printed by permission from Oxford University Press Annals of Botany Nanoparticles as Smart Treatment-delivery Systems in Plants: assessment of different techniques of Microscopy for their Visualization in Plant Tissues, González-Melendi et al. [52]. Copyright © 2007. https://doi.org/10.1093/aob/mcm283

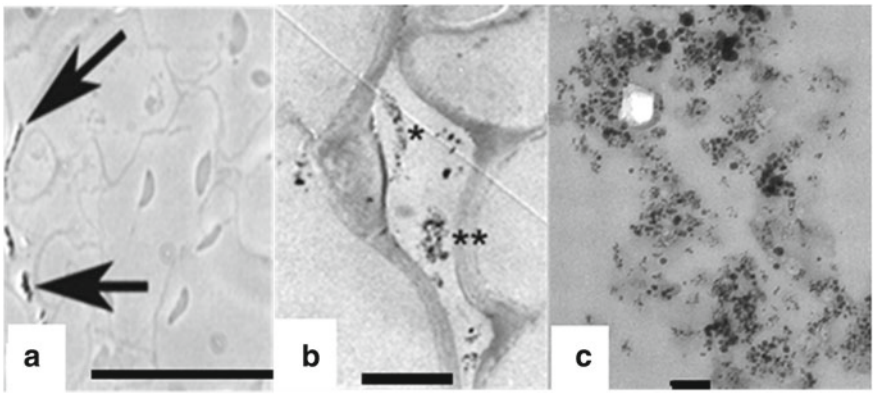

Fig. 13.5 **a** Phase contrast light microscope image of a string of nanoparticles (pointed by arrows) along the cells on the outer side of the cell wall at the epidermis. **b** TEM image of nanoparticle aggregates, marked with asterisks. **c** TEM magnification of the aggregate marked with two asterisks. in **b** The same Scale bars: 50 μm, 5 μm and 0.1 μm, respectively. Printed by permission from Oxford University Press Annals of Botany Nanoparticles as Smart Treatment-delivery Systems in Plants: assessment of different techniques of Microscopy for their Visualization in Plant Tissues, González-Melendi et al. Copyright © 2007. https://doi.org/10.1093/aob/mcm283

smallest population. The majority of the observed nanoparticles has a diameter equal or below 10 nm. In solution, these nanoparticles form aggregates with a diameter ranging from 5 to 200 nm [61]. The fact that no particles bigger than 50 nm were detected in the plant tissues suggest a size selection mechanism (maybe due to the cell walls and waxes), although more studies are necessary to clarify the nanoparticles penetration mechanisms in their movement to and through the plant vascular system.

The observation of all the samples taken from different points of the plant and at different time intervals, suggests that the nanoparticles move from the point of application progressively penetrating the different tissues of the plant. Analyzing samples taken near the application point, aggregates of nanoparticles were detected in the internal wall of the pit cavity (see Fig. 13.2 right) at the point of administration 24 h after injection, and 48 h after administration these nanoparticles had migrated into the stem parenchima. It is significant that these aggregates appeared in adjacent cells forming chains (with 2–5 cells) between the vascular cores and radially oriented to the stem surface, suggesting than the nanoparticles move from cell to cell. It seems unlikely that in this movement the aggregates of nanoparticles enter directly into cytoplasm; therefore, it is most likely that the nanoparticles enter individually, and aggregate spontaneously once inside the cell. Some aggregates were also visualized in the extracellular space between cells. Results also showed the presence of nanoparticles in the outer surface of the plant, both inside and outside of the trichomes, 24 h after application. This fact indicates that at least part of the nanoparticle suspension was expelled in a short time, as if the plant got rid of the excess of nanoparticles, maybe as a kind of detoxification mechanism. At 48 h nanoparticle aggregates were

also observed inside the xylem vessels. After 168 h there were almost no nanoparticles, neither in the pit cavity, nor in the tissues of the stem near the point of application. TEM analysis of samples collected 48 h after the administration, close to the magnets placed far from the point of injection, revealed the presence of individual nanoparticles in the cytoplasm of cells close to the vascular system. Nanoparticles were also observed inside the xylem vessels, suggesting that the nanoparticles use them for travelling long distances inside the plant. The microscopy study carried out in the different samples allowed also to analyze the structure of the cytoplasm. A dense cytoplasm with starch-containing organelles was observed in those cells collected 24 h after injection, with nanoparticle aggregates in the cytosol. However these starch structures were neither detected in adjacent cells without nanoparticles, nor in the cytoplasm of cells in tissues collected far from the application point 48 h later, containing individual nanoparticles. This fact suggests that these changes in their subcellular organization could be a plant response to the presence of a high density of nanoparticles. Cytotoxicity has been associated with the dose of nanoparticles [65], in particular with those in a magnetic ferrofluid [66–68]. However, only with our experiments it is not possible to assess if the observed reaction to the Fe@C nanoparticles is specific of the plant cells, or is a common cell reaction to high nanoparticle concentrations in the cytoplasm. Moreover, an effect of the calcium in the gelafundine in which nanoparticles are suspended cannot be completely excluded.

13.2.2 Nanoparticle Application by Spray

This methodology was chosen because is more similar to that used by agronomists in cultivated plants, for example for phytosanitary control. The experiments were as well carried out on living pumpkin plants and with the Fe@C nanoparticles suspended in gelafundine [52]. Drops of nanoparticle suspension were sprayed of the surface of leaves close to the insertion of the petiole. Tissue samples (close and far from the application point) were also collected 24, 48 and 168 h after spraying. In this case, nanoparticles were only observed in samples taken 168 h after application. It was not possible to distinguish any nanoparticle aggregates by light microscopy, and the nanoparticles were only visible in TEM images of cells from the epidermis of the petiole close to the application point. Moreover, there were no nanoparticles in cells beyond the first epidermal layer. In these cells the nanoparticles appeared isolated, not in aggregates. There was no difference between the intracellular structure density observed in those cells with nanoparticles and in the neighboring cells without nanoparticles in their cytoplasm. As the epidermic outer cell wall has a considerable thickness and is covered by protective waxes, it is quite likely that the nanoparticles penetrate through the stomata and the subestomatic chambers. In fact, this is a route used by pathogens of different species [69, 70]. The fact that nanoparticles passed through the epidermal cell wall opens up the possible application of these nanotechnology tools for agronomical purposes. However, these results should be taken as preliminary. For example, the fact that the amount of nanoparticles found in

the tissue samples was less than that found when applying the nanoparticles by injection, raises the need to optimize the suspension of nanoparticles, testing for example other biocompatible liquid carriers, functionalized nanoparticles for a higher affinity with the leave tissues etc.

13.2.3 Nanoparticle Application by the Roots

The study on the nanoparticle absorption and translocation was extended to the case in which the nanoparticles penetrate through the roots into the plant. In this case no magnets were used, to study the free movement of the nanoparticles inside the plant. A comparative analysis was carried out in four living crop plants belonging to different families, to unveil whether there were differences regarding the transport routes, the organs and tissues where nanoparticles tend to accumulate. This research was carried out on sunflower (*Helianthus annuus*) from the family *Compositae*; tomato (*Lycopersicum sculentum*) from the *Solanaceae*; pea (*Pisum sativum*), from the *Fabaceae*; and wheat (*Triticum aestivum*), from the *Triticeae* [55]. In this case, the plants were grown in vitro using a Petri dish system (rhizotron) allowing the visualization of the roots [71]. A biocompatible magnetic fluid was prepared suspending the Fe@C nanoparticles in manitol solution (1%). Once the plants developed the second pair of leaves some of the roots were immersed in the suspension (see Fig. 13.6a). Tissues

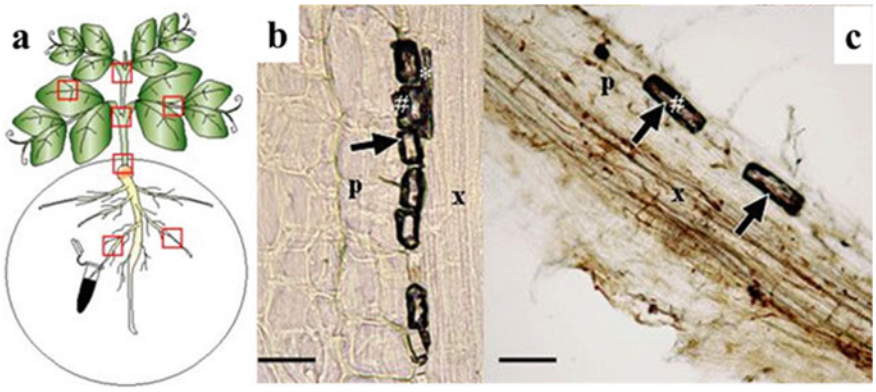

Fig. 13.6 Scheme of the plant showing the nanoparticle administration procedure and the tissue sections for microscopy analysis. **a** Root longitudinal sections of pea **b** and sunflower. **c** Samples were taken 24 h after nanoparticle administration. Arrows point to nanoparticle accumulations. Symbols # and * indicate cells from the parenchyma (p) and from the xylem (x), respectively. Scale bars are 25 μm in **b** and 50 μm in (**c**). Reprinted by permission from Springer Nature Customer Service Centre GmbH: Springer Nature Journal of Nanobiotechnology Absorption and traslocation to the aerial part of magnetic carbon-coated nanoparticles through the root of different crop plants Cifuentes et al. [55]. Copyright © 2010. https://doi.org/10.1186/1477-3155-8-26

from different parts of the plants were taken after 24 and 48 h, from the sections drawn in (Fig. 13.6a, and fixed for conventional light microscope analysis.

Big amounts of nanoparticles (in the form of a black staining corresponding to nanoparticle aggregates) were observed in samples of root tissue collected after 24 h (see Fig. 13.6b, c). These observations led to the conclusion that nanoparticle application by immersing the roots into the nanoparticle solution is faster, more reliable and efficient (in terms of the amount of nanoparticles) than application by pulverization or injection [52, 54]. This conclusion is common to the four crops analyzed in this study. Although in all cases nanoparticles were easily detected in the xylem vessels, some differences were observed depending on the species. Pea roots accumulated higher contents of nanoparticles than sunflower or wheat, for example. This difference still remained after 48 h of exposure to the nanoparticle fluid, suggesting that pea roots could be more permeable to nanoparticle penetration. Looking for the presence of nanoparticles in roots not exposed directly to the suspension, the characteristic black deposit was detected within the central cylinder of roots located diametrically opposite to the treated roots. Therefore, the nanoparticles had moved there probably through the phloem and using the source-sink pressure gradient [72]. This is also in good agreement with the observations in pumpkin plants with respect to the radial transport of nanoparticles from cell to cell [52, 54].

The translocation of the nanoparticles into the aerial parts of the plant was also studied, taking tissue samples from the plant crown 24 and 48 h after nanoparticle application. After 24 h the black deposit was observed in the xylem vessels of the four crops as shown in Fig. 13.7a–d, which means that the nanoparticles had quickly moved most likely by the transpiration stream.

As in the case of the roots, there were differences between species. Pea and wheat showed a high concentration of nanoparticles in the vascular tissues of the crown, whereas the black staining was less intense in tomato and sunflower. In the case of sunflower, it seems that the nanoparticle uptake through the roots is much slower than in the other species, and for that reason there is a lower accumulation after 24 h of nanoparticle treatment. In addition, in this case the nanoparticle suspension seems to be more restricted to the vascular tissues than in the other species. The observation of subsequent upper part sections confirmed that nanoparticles reached most of them also after 24 h of exposure to the suspension. The samples taken 48 h after nanoparticle application (see Fig. 13.7e–j) showed no significant differences from crop to crop, as an intense accumulation of nanoparticles was detected in all the cases. According to the microscopy analysis, the nanoparticles moved also towards the leaves and leaf petioles. Another striking result is that large accumulations of nanoparticles were detected in the leaf trichomes of the wheat plants, but not in the other three crop species. As mentioned in previous sections, the same was observed in pumpkin plants [52, 54], although not in such a high amount. This fact would confirm the secretory function of the trichomes [73], being this a putative detoxifying pathway. Different behavior regarding accumulation and excretion of heavy metals has been reported for different plant species [74], suggesting that such differences can also be found when working with metal nanoparticles. The reasons for the observed differences between crops are unclear, but they should be related to the physiology

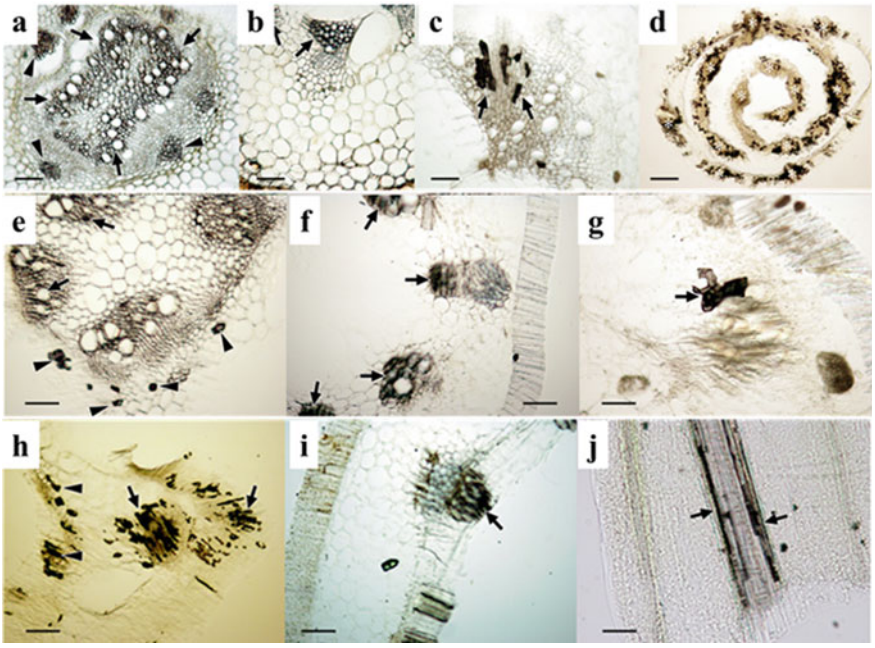

Fig. 13.7 Tissues from the crown of pea **a**, sunflower **b**, tomato **c** and wheat **d** cut 24 h after suspension administration. Detail of the first internode cross section of pea **e**, sunflower **f** and tomato **g** 48 h after suspension administration. Detail of the second internode cross section of pea **h**, sunflower **i** and wheat **j** 48 h after suspension administration. Scale bars in images (a)-**i** correspond to 100 μm; scale bar in images **j** corresponds to 50 μm. Reprinted by permission from Springer Nature Customer Service Centre GmbH: Springer Nature Journal of Nanobiotechnology Absorption and traslocation to the aerial part of magnetic carbon-coated nanoparticles through the root of different crop plants Cifuentes et al. [55]. Copyright © 2010. https://doi.org/10.1186/1477-3155-8-26

of the plants: wheat belongs to the monocot plant group, whereas the other three crops are dicots.

Therefore, these results and those obtained in pumpkin plants have shown that biocompatible nanoparticle suspensions can be administered to whole living plants, can circulate through their vascular system, either by themselves or by applying magnetic field gradients, and can also be located on specific places, from the root to the aerial parts. The study carried out by different microscopy techniques has allowed the accurate visualization of nanoparticles in tissues and cells. However, more detailed studies at cell level, including HR-TEM, are necessary to clarify the mechanisms by which nanoparticles can penetrate into the plant cells, as this is currently a controversial subject. In addition, special attention has to be paid to toxicity studies. In the work with pumpkin plants, some of the specimens treated with nanoparticles were transplanted to pots where they continued to grow, and no damage was observed. However, these results should be viewed with caution because it has been reported that in in vitro treatments [66–68], nanoparticles may cause some

local damage at cell level. Moreover, as cyto- and phyto-toxicity are dose-dependent, they cannot be discarded in case of treatments with more concentrated nanoparticle suspensions.

13.3 Interaction of Silica Coated Magnetic Nanoparticles with Pathogenic Fungi

In this section, the study of the interaction between silica coated iron oxide ($Fe_3O_4@SiO_2$) nanoparticles and fungal cells is presented, paying attention to the affinity and internalization of the particles by hyphal cells, and to their toxicity [48].

The core-shell nanoparticles were synthesized in two steps. First, the magnetite core was synthesized by coprecipitation, as described in De Matteis et al. [75]. According to the X-ray diffraction pattern and HR-TEM images of the synthesized powders, the nanoparticles were mainly composed by magnetite and only in some batches a small fraction of maghemite was detected. The particles were subsequently coated with an aminated silica shell and functionalized with protein G following the protocols reported in [47]. The diameter of the silica-coated nanoparticles was about 50–100 nm. The protein G on the surface was afterwards conjugated to AlexaFluor488, to visualize the nanoparticles by confocal microscopy when studying their interaction with the Fusarium. In addition, when the nanoparticles were going to be used for sensing purposes, the protein G would easily allow their further conjugation with the biomolecule that specifically recognizes the pathogenic fungus [47]. All the experiments described from here on were carried out on *F. oxysporum forma specialis lycopersici*. The fungal strain was stored as microconidial suspension in 30% glycerol at −80 °C. For microconidia production, cultures were grown in potato dextrose broth [48].

13.3.1 Internalization of $Fe_3O_4@SiO_2$ Nanoparticles by Fungal Cells

First of all, the affinity between the $Fe_3O_4@SiO_2$ nanoparticles and the fungus was studied. With this purpose, turbidity (or relative absorbance) measurements were performed on conidial suspensions incubated with magnetic nanoparticles, after different incubation times. In all the cases, 5×10^6 microconidia were grown for 16 h at 28 °C under agitation at 170 rpm in 1 mL of minimum medium (MM) [76]. The measurements were performed after long-term and short-term incubation experiments. In the first case the conidia were grown in MM supplemented with nanoparticles at 200 $\mu g\ ml^{-1}$. In short-term incubation experiments, conidia were grown in the absence of nanoparticles. They were added to the MM after 16 h of conidia growth and incubated there for 5 s, 15 min and 30 min. After incubation with

the nanoparticles, the suspensions were filtered to remove nanoparticles not internalized/not attached in/to the conidia, and the filtrate was resuspended in new fresh MM. This suspension was introduced in a magnetic separator, and kept under the action of the magnetic field for 1, 3 and 5 min. At these times, an aliquot of the medium was taken for turbidity measurements. All those fungi attached to the magnetic nanoparticles were going to be trapped by the magnet, decreasing the conidia concentration in the aliquot, and consequently, decreasing its turbidity. The optical density of this aliquot was measured at 600 nm (A600), and compared with the absorbance of a control sample (a sample not introduced in the magnetic separator). The reduction in absorbance was correlated with the nanoparticle attachment/internalization in/to the fungus. After long-term incubation with magnetic nanoparticles, the conidia were attracted by the magnet as early as 1 min after being introduced in the magnetic separator, and the turbidity of the medium was reduced dramatically, confirming the attachment of the nanoparticles to the hyphae. The long-term incubation experiments were also performed with the $Fe_3O_4@SiO_2$ nanoparticles after their functionalization with protein G, to verify whether the protein influenced the fungus-nanoparticle interaction. In fact, the functionalization of the nanoparticle surface delayed the particle movement towards the magnet, although a turbidity decrease similar to that observed when working with the non-functionalized nanoparticles was detected after 5 min. Short-term incubation experiments were also performed incubating the grown conidia with functionalized and non-functionalized $Fe_3O_4@SiO_2$ nanoparticles. The turbidity measurements were carried out following the protocol described above for long term experiments. A drastic reduction of the turbidity was observed after incubating fungal conidia with both functionalized and non-functionalized nanoparticles for as short as 5 s. These results evidence the high affinity of the functionalized and non-functionalized $Fe_3O_4@SiO_2$ nanoparticles for the fungal hyphae.

In order to investigate whether the nanoparticles were able to penetrate the fungal hypha or remained attached to its surface, visible, confocal and transmission electron (TEM) microscopies on conidia cultures after long-term and short-term incubation with $Fe_3O_4@SiO_2$ nanoparticles were carried out. For these studies, 5×10^6 conidia were grown for 16 h at 28 °C under agitation at 170 rpm in 1 ml of MM. For long-term studies, 200 $\mu g\ ml^{-1}$ of nanoparticle suspension was added at the time of fungus inoculation, while for short-term studies the nanoparticles were added to MM after 16 h growth and incubated for either 10 min or 3 h before visualization. First of all, confocal images of thin time-course confocal optical sections (~1 μm thick) were acquired. Details about the microscope and the instrumental conditions can be found in [48]. The results are displayed in Fig. 13.8. After 10 min of incubation, fluorescent $Fe_3O_4@SiO_2$ nanoparticle aggregates attached to the fungal hyphal surfaces were clearly seen (pointed by an arrow head at visible field and stack projection in Fig. 13.8a). However, theses aggregates did not penetrate the fungal hyphae since 3D optical sections showed a clear signal only for the largest aggregates attached to the hypha. Although the penetration of non-aggregated nanoparticles could not be inferred from the confocal images, it cannot be discarded. After 16 h of incubation, nanoparticle aggregates were still visible and attached on the hyphal surface, although they were smaller than those attached after 10 min incubation, and no signal

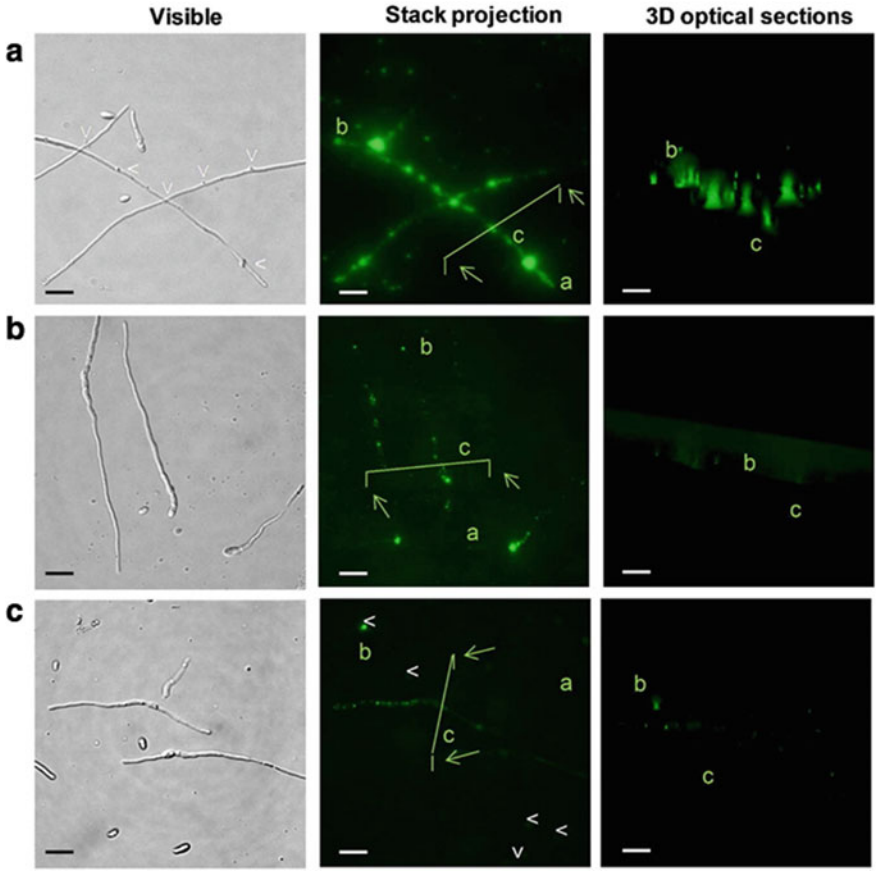

Fig. 13.8 Visible and confocal micrographs of overview images (stack projections) and the transverse optical section of *F. oxysporum* incubated with Fe_3O_4@SiO_2 nanoparticles for 10 min **a**, and 16 h **b**, and of the filtered sample re-suspended for 4 h in fresh MM **c**. The orientation of the images is indicated by lower case letters, for ease of understanding. *T* plane of the section shown in the 3D images is indicated by the green hurdle in the overview. Scale bars correspond to 10 μm. Reprinted with permission from Rispail et al. [48]. https://doi.org/10.1021/am501029gCopyright © 2014 American Chemical Society

was observed in the 3D optical sections (Fig. 13.8b). The eventual detachment of the nanoparticles from the fungal cells was also studied. With this purpose 16 h conidial suspensions already incubated with nanoparticles were filtered through a 0.45 μm filter to remove all the nanoparticles that could be in the medium, not attached to the hypha. The filtered sample was re-suspended in sterile MM for 4 h at 28 °C. Confocal images taken afterwards (Fig. 13.8c, arrow heads) showed that after 4 h some aggregates remained in the hypha, although some of them detached and were suspended in de medium.

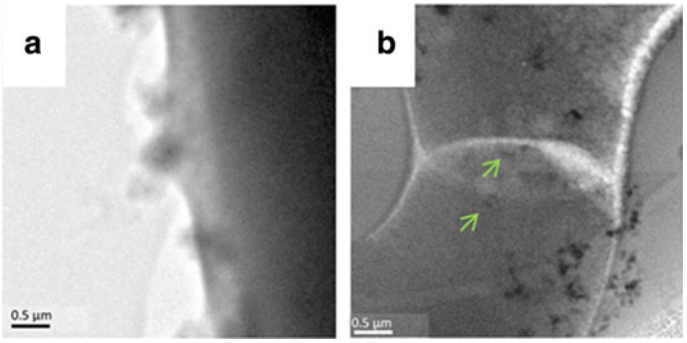

Fig. 13.9 BF-TEM image showing a detail of a *F. oxysporum* hypha **a** and a detail of the hyphal septum. **b** Arrows point to nanoparticles in the septum. Scale bars correspond to 0.5 µm. Adapted with permission from Rispail et al. [48]. https://doi.org/10.1021/am501029g. Copyright 2014 American Chemical Society

The confocal microscopy study was completed by TEM and Scanning Transmission Electron Microscopy-High Angle Annular Dark Field (STEM-HAADF) observation in a Tecnai F30 (FEI), operated at 300 kV. Samples were carefully prepared following cryo-TEM protocols [48]. Bright field (BF)-TEM images taken after 16 h incubation showed a range of small to medium aggregates corresponding to the $Fe_3O_4@SiO_2$ nanoparticles attached to the fungal surface and some individual nanoparticles moving through the fungal cell wall, as shown in Fig. 13.9a. Careful observations near to the fungal septum (see Fig. 13.9b) suggested that few individual nanoparticles (pointed by arrows in the figure) could enter the fungal cells. This assumption was also supported by focal series of STEM-HAADF images.

The chemical composition of the aggregates was analyzed by STEM-HAADF (see Fig. 13.10a, b) and Dispersive X-Ray Spectroscopy (EDS). The EDS spectra as the ones presented in Fig. 13.10c, d confirmed that the nanoparticles consist of an iron oxide core coated by a SiO_2 shell.

The fact that only a small fraction of individual nanoparticles penetrated the fungal cells whereas a large fraction of particles remain attached to the hypha coincides with the results obtained by confocal microscopy. This makes a difference with other nanomaterials, such as quantum dots. A similar study carried out in the same *forma specialis* of *F. oxysporum* indicated that quantum dots penetrate in a much larger amount into the cell [48]. As cellular uptake is closely related to the physicochemical properties of the nanosized objects, the different behavior of the quantum dots and the $Fe_3O_4@SiO_2$ nanoparticles in this study could be due to the different size of both nanomaterials (13–15 nm in the case of quantum dots versus 50–100 nm in the case of nanoparticles). In addition, although both nanomaterials were incubated together with the fungal conidia in MM at the same pH, their respective surface charge was different (approximately -35 mV in the case of quantum dots and about +25 mV the one of the nanoparticles). This different sign would determine the interaction with the proteins of the fungal cell wall characteristic of hyphal cells. The

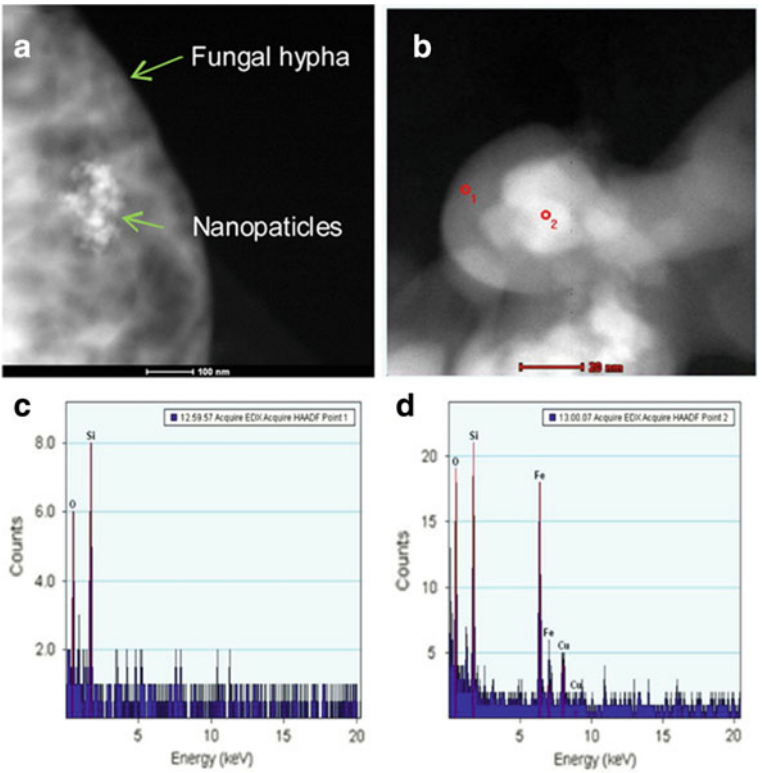

Fig. 13.10 STEM-HAADF images of a Fe_3O_4@SiO_2 nanoparticle aggregate adhered to a fungal hypha **a** and of a nanoparticle **b**. Here the o1 and o2 spots correspond to the EDS spectra shown in **c** and **d**. Scale bars in **a** and **b** represent 100 and 20 nm, respectively. Reprinted with permission from Rispail et al. [48]. https://doi.org/10.1021/am501029g. Copyright © 2014 American Chemical Society

outer layer of the cell wall of *F. oxysporum* is enriched in glycoproteins [77]. Since the glycoproteins are negatively charged, they will attract the positively charged nanoparticles by electrostatic interactions. This would favor the formation of the observed large nanoparticle aggregates, large enough to be observed in the confocal and even visible field. This large size might as well hamper their uptake. In addition, the images taken after the longest incubation periods showed that the number of aggregates decreased with time. This fact could be ascribed to the increase in the acidification of the incubation medium during *F. oxysporum* growth [78], that might increase the nanoparticle surface charge and in turn improve the stability of the isolated nanoparticles.

13.3.2 *Fe_3O_4@SiO_2 Nanoparticle Toxicity on* F. Oxysporum *Hyphal Cells*

The experiments performed to outline the toxicity profile of the synthesized Fe_3O_4@SiO_2 nanoparticles included colony growth assessment, the study of the reactive oxygen species (ROS) accumulation and oxidative stress, and the study of the fungal cell viability. In each case microconidia were grown in MM supplemented with nanoparticle concentrations equal to 25, 50, 100 and 500 $\mu g\ ml^{-1}$. The results demonstrated the low toxicity of the nanoparticles to these *forma specialis*, even at the highest nanoparticle concentration.

The experiments described above show that, although the fraction of Fe_3O_4@SiO_2 nanoparticles that penetrate the hypha is not very large, they remain as magnetic aggregates adhered to the fungus surface, which is already enough to be separated magnetically and to be detected by the magnetic reader of a biosensor. In addition, these nanoparticles in usual working doses are per se not toxic, so in principle they are not harmful to other non-pathogenic/beneficial fungi that may exist in the environment. This research constitutes the stage before the functionalization of the nanoparticles for the detection of the pathogen and also paves the way for the search of other biomolecules or active principles that could also be housed on the nanoparticle surface. This would result in multifunctional nanoparticles that could be used not only for detection, but also for the selective control and eventual elimination of the pathogenic fungus.

13.4 Summary and Persperctives

The work presented here evidences that magnetic nanoparticles are very attractive nanomaterials to be considered in research related to Life Sciences areas different from those more explored up to now, as the ones directly connected to Bio-medicine. The results presented here show how these nanosystems can be very useful, first of all, for basic research, to study the fundamental problems concerning their interaction with plants and microorganisms. In addition, these studies open the way to solve a large list of practical problems in agriculture, agronomy, environment, biotechnology, food industry, etc., which in the short and/or long term also influence health, quality of life and global welfare.

The work carried out with the Fe@C nanoparticles has shown that these nanoparticles are very appropriate for *in-planta* application and for plant cell research. First, because they are suitable for the synthesis of different biocompatible magnetic fluids easy to administer to living whole plants by different routes (injection, spray and immersion of the roots in the fluid). Second, they have an adequate response to magnetic field gradients. This characteristic, together with the high porosity and high specific surface area of their coating makes them very appropriate as magnetically responsive carriers for the localized delivery of different chemical substances,

such as those used in phytosanitary treatments, for pest control, etc. Although there are still many problems to be solved for their large-scale use, the work presented here can help in preliminary studies at laboratory scale (for instance, in those necessary for the optimization of the routes and doses to be administered in a specific treatment). Regarding their use in the laboratory, the Fe@C nanoparticles have been found as very convenient when working with plants and plant cells, as they are very easy to be visualized (without the need of any extra marker) by the microscopy techniques and protocols that have been developed during the execution of the different experiments. Therefore, the Fe@C magnetic nanoparticles can be of great help in elucidating the penetration mechanisms and the localization of the nanoparticles into the cell (for instance, by HR-TEM experiments) as well as the cell response to the nanocarriers. These topics are currently under discussion and are of great importance from the point of view of both basic and applied research (for example for the case of genetic engineering). Moreover, cell viability and cytotoxicity assays as well as the study of the relationship between cytotoxicity and phytotoxicity are of paramount importance prior their use in practice.

The use of magnetic nanoparticles coated with silica is much more exploited than that of the other magnetic nanoparticles. Their widespread implementation in biomedical applications has stimulated the rapid growth that their utilization in areas such as biotechnology, agriculture and agronomy is currently experiencing. The previous section summarizes what constitutes a systematic study of the interaction of $Fe_3O_4@SiO_2$ nanoparticles with a fungus that in one of its *forma specialis* is a plant pathogen and even an opportunistic human pathogen. One aspect that this work has highlighted is the importance of the physicochemical properties of the nanoparticles that have to be precisely tuned for each particular application. In this particular case, the size of the nanoparticles and their electrical charge has been determinant for their application in a biosensor that detects and allows the separation of the pathogenic fungus from infected soils, plants and crops. In particular, the different sign of the charge of the fungal cell wall of these hyphal cells and that of the silica coating causes the nanoparticles to be located in the form of relatively large magnetic aggregates on the fungal hypha. This has turned out to be decisive for the development of the future device, facilitating the detection and subsequent magnetic separation of the pathogen. Therefore, in the same way as for a given cell model it is necessary to know the toxicity profile of a particular nanomaterial, an exhaustive characterization of the physicochemical properties of this nanomaterial is also essential. At present, nanotechnology offers us advanced characterization techniques (which include magnetic characterization techniques, advanced microscopy, different spectroscopies etc.) that are more and more intended for the characterization of materials of biological interest, as well as biomaterials. In addition, the methodology and protocols developed for the case of the silica coated nanoparticles interacting with *Fusarium oxisporum* might then be implemented in the detection and control of other pathogens and pests, which would have a major impact on areas such as agronomy and agriculture, food industry etc. Moreover, this study could be extended to other fungi that are or can become pathogenic for humans, as for example those of *Candida* genus. Just as the resistance to antibiotics developed by bacteria

is a serious problem and is the cause of many deaths, certain pathogenic fungi have also become resistant to antifungals, and hence, there are fewer and fewer effective treatments. This opens a wide research field, and the fact that Nanoscience and Nanotechnology could contribute to finding solutions for their treatment and definitive elimination would represent a great benefit for the patient health In addition, the treatment of hospital acquired infections represents one of the highest costs of the health system and therefore, the solution to these problems would be enormously beneficial, also from the economic point of view.

When working with nanoparticles for applications as the ones discussed here, that involve plants and microorganisms present in our environment, it is essential to keep in mind that particles could in principle enter the food chain of animals and humans, with the consequent health impact. Therefore, before putting these ideas into practice, an exhaustive assessment of the nanoparticle fate is necessary, studying their degradability, their accumulation in fruits, seeds, roots, etc., and their possible excretion and effects on soils. Rigorous toxicity and ecotoxicity studies, leading to standardized nanorisk assessment protocols are mandatory. All this will contribute to improving the public perception of these new advances, and making people more confident about the use of new products based on nanotechnology.

Acknowledgements The author wish to thank the following colleagues: M. R. Ibarra, R. Fernández-Pacheco, D. Serrate, Z. Cifuentes, M. J. Coronado, E. Corredor, L. Custardoy, L. De Matteis, P. Fevereiro, J. M. de la Fuente, P. González-Melendi, C. Maycock, A. S. Miguel, A. Oliva, A. Pérez de Luque, E. Prats, N. Rispail, M. C. Risueño, D. Rubiales, R. Santos and P. S. Testillano. Financial support from the Spanish Ministerio de Economía y Competitividad (MINECO) through project MAT2016-78,201-P, and from the Department of Innovation, Research and University of the Government of Aragon through the Research Groups grants program co-financed by the FEDER Operational Program Aragón 2014–2020 "Building Europe from Aragon", is also acknowledged. The author also thanks the following publishers and journals: Springer Nature BMC Plant Biology (https://bmcplantbiol.biomedcentral.com/), as the original source of Fig. 13.2 published in Corredor et al. 2009, https://doi.org/10.1186/1471-2229-9-45; Oxford University Press Annals of Botany (www.aob.oxfordjournals.org), as original source of Figs. 13.3, 13.4 and 13.5, published in González-Melendi et al. 2008, https://doi.org/10.1093/aob/mcm283; BioMed Central Journal of Nanobiotechnology (https://jnanobiotechnology.biomedcentral.com/), as the original source of Figs. 13.6 and 13.7, published in Cifuentes et al. 2010. https://doi.org/10.1186/1477-3155-8-26; and American Chemical Society ASC Applied Materials and Interfaces, as the original source of Figs. 13.8, 13.9 and 13.10, published in Rispail et al. ACS Appl. Mater. Interfaces, 2014, 6 (12), pp 9100–9110 https://doi.org/10.1021/am501029g.

References

1. F. Torney, B.G. Trewyn, V.S.Y. Lin, K. Wang, Nat. Nanotechnol. **2**, 295 (2007)
2. S. Martin-Ortigosa, J.S. Valenstein, W. Sun, L. Moeller, N. Fang, B.G. Trewyn, V.S.Y. Lin, K. Wang, Small **8**, 413 (2012)
3. S. Martin-Ortigosa, J.S. Valenstein, V.S.Y. Lin, B.G. Trewyn, K. Wang, Adv. Func. Mater. **22**, 3576 (2012)
4. S. Martin-Ortigosa, D.J. Peterson, J.S. Valenstein, V.S.Y. Lin, B.G. Trewyn, L.A. Lyznik, K. Wang, Plant Physiol. **164**, 537 (2014)

5. A.T. Silva, N. Alien, C.M. Ye, J. Verchot, J.H. Moon, BMC Plant Biol. **10**, 291 (2010)
6. L. Jiang, L. Ding, B.C. He, J. Shen, Z.J. Xu, M.Z. Yin, X.L. Zhang, Nanoscale **6**, 9965 (2014)
7. H.W. Xun et al., Environ. Pollut. **229**, 479 (2017)
8. F.H. Hong, J. Zhou, C. Liu, F. Yang, C. Wu, L. Zheng, P. Yang, Biol. Trace Elem. Res. **105**, 269 (2005)
9. L. Zheng, F.S. Hong, S.P. Lu, C. Liu, Biol. Trace Elem. Res. **104**, 83 (2005)
10. T.P. Frazier, C.E. Burklew, B.H. Zhang, Funct. Integr. Genomics **14**, 75 (2014)
11. D.H. Lin, B.S. Xing, Environ. Pollut. **150**, 243 (2007)
12. D.H. Lin, B.S. Xing, Environ. Sci. Technol. **42**, 5580 (2008)
13. A. Perez de Luque, D. Rubiales, Pest Manag. Sci. **65**, 540 (2009)
14. A. Servin, W. Elmer, A. Mukherjee, R. De la Torre-Roche, H. Hamdi, J.C. White, P. Bindraban, C. Dimkpa, J. Nanopart. Res. **17**, 92 (2015)
15. F. Yasmeen, N.I. Raja, A. Razzaq, S. Komatsu, Biochimica Et Biophysica Acta-Proteins and Proteomics **1865**, 28 (2017)
16. D.L. Graham, H.A. Ferreira, P.P. Freitas, Trends Biotechnol. **22**, 455 (2004)
17. C. Marquina, J.M. de Teresa, D. Serrate, J. Marzo, F.A. Cardoso, D. Saurel, S. Cardoso, P.P. Freitas, M.R. Ibarra, J. Magn. Magn. Mater. **324**, 3495 (2012)
18. D. Serrate, J.M. De Teresa, C. Marquina, J. Marzo, D. Saurel, F.A. Cardoso, S. Cardoso, P.P. Freitas, M.R. Ibarra, Biosens. Bioelectron. **35**, 206 (2012)
19. B. Sepulveda, P.C. Angelome, L.M. Lechuga, L.M. Liz-Marzan, Nano Today **4**, 244 (2009)
20. Z.M. Liu, X.Y. Xia, C.Y. Yang, L. Wang, Rsc Advances **5**, 100891 (2015)
21. L. Wang, Z.M. Liu, X.Y. Xia, J.Y. Huang, Anal. Methods **8**, 6959 (2016)
22. D. Giust, M.I. Lucio, A.H. El-Sagheer, T. Brown, L.E. Williams, O.L. Muskens, A.G. Kanaras, ACS Nano **12**, 6273 (2018)
23. U. Kadam, C.A. Moeller, J. Irudayaraj, B. Schulz, Plant Biotechnol. J. **12**, 568 (2014)
24. U.S. Kadam, B. Schulz, J.M.K. Irudayaraj, Plant Journal **90**, 1187 (2017)
25. V.K. Sharma, R.A. Yngard, Y. Lin, Adv. Coll. Interface. Sci. **145**, 83 (2009)
26. Y.K. Jo, B.H. Kim, G. Jung, Plant Dis. **93**, 1037 (2009)
27. S. Gurunathan, J.W. Han, D.N. Kwon, J.H. Kim, Nanoscale Res. Lett. **9**, 373 (2014)
28. S. Banik, A. Perez-de-Luque, Spanish Journal of Agricultural Research **15**, e1005 (2017)
29. A. Sirelkhatim, S. Mahmud, A. Seeni, N.H.M. Kaus, L.C. Ann, S.K.M. Bakhori, H. Hasan, D. Mohamad, Nano-Micro Letters **7**, 219 (2015)
30. N. Padmavathy, R. Vijayaraghavan, Sci. Technol. Adv. Mater. **9**, 035004 (2008)
31. T. Jin, Y.P. He, J. Nanopart. Res. **13**, 6877 (2011)
32. Y.H. Leung et al., Small **10**, 1171 (2014)
33. I.F. Castillo, L. De Matteis, C. Marquina, E. García Guillén, J.M. de la Fuente, S. G. Mitchell, Int. Biodeterior. Biodegradation **141**, 79 (2018)
34. C. Alexiou, W. Arnold, R.J. Klein, F.G. Parak, P. Hulin, C. Bergemann, W. Erhardt, S. Wagenpfeil, A.S. Lubbe, Can. Res. **60**, 6641 (2000)
35. R. Fernandez-Pacheco et al., J. Magn. Magn. Mater. **311**, 318 (2007)
36. H. Van As, T. Scheenen, F.J. Vergeldt, Photosynth. Res. **102**, 213 (2009)
37. T. Scheenen, A. Heemskerk, A. de Jager, F. Vergeldt, H. Van As, Biophys. J. **82**, 481 (2002)
38. T.W.J. Scheenen, F.J. Vergeldt, A.M. Heemskerk, H. Van As, Plant Physiol. **144**, 1157 (2007)
39. C. Hillnhutter, R.A. Sikora, E.C. Oerke, D. van Dusschoten, J. Exp. Bot. **63**, 319 (2012)
40. V. Grazu, A.M. Silber, M. Moros, L. Asin, T.E. Torres, C. Marquina, M.R. Ibarra, G.F. Goya, Int. J. Nanomed. **7**, 5351 (2012)
41. F.G. Aliev, M.A. Correa-Duarte, A. Mamedov, J.W. Ostrander, M. Giersig, L.M. Liz-Marzan, N.A. Kotov, Adv. Mater. **11**, 1006 (1999)
42. R. Fernandez-Pacheco, M. Arruebo, C. Marquina, R. Ibarra, J. Arbiol, J. Santamaria, Nanotechnology **17**, 1188 (2006)
43. C. Gruttner, S. Rudershausen, J. Teller, J. Magn. Magn. Mater. **225**, 1 (2001)
44. H. Pardoe, W. Chua-anusorn, T.G. St Pierre, J. Dobson, J. Magn. Magn. Mater. **225**, 41 (2001)
45. A. Zahr, C. Davis, M. Pishko, Langmuir **22**, 8178 (2006)

46. M. Arruebo, R. Fernandez-Pacheco, B. Velasco, C. Marquina, J. Arbiol, S. Irusta, M.R. Ibarra, J. Santamaria, Adv. Func. Mater. **17**, 1473 (2007)
47. R. Arenal, L. De Matteis, L. Custardoy, A. Mayoral, M. Tence, V. Grazu, J.M. De La Fuente, C. Marquina, M.R. Ibarra, ACS Nano **7**, 4006 (2013)
48. N. Rispail et al., ACS Appl. Mater. Interfaces. **6**(12), 9100–9110 (2014)
49. C. Barbe, J. Bartlett, L.G. Kong, K. Finnie, H.Q. Lin, M. Larkin, S. Calleja, A. Bush, G. Calleja, Adv. Mater. **16**, 1959 (2004)
50. J.M. De Teresa, C. Marquina, D. Serrate, R. Fernandez-Pacheco, L. Morellon, P.A. Algarabel, M.R. Ibarra, Int. J. Nanotechnol. **2**, 3 (2005)
51. E. Escribano, R. Fernandez-Pacheco, J. Valdivia, M. Ibarra, C. Marquina, J. Queralt, Arch. Pharmacal Res. **35**, 93 (2012)
52. P. Gonzalez-Melendi et al., Ann. Bot. **101**, 187 (2008)
53. A.A. Kuznetsov, V.I. Filippov, O.A. Kuznetsov, V.G. Gerlivanov, E.K. Dobrinsky, S.I. Malashin, J. Magn. Magn. Mater. **194**, 22 (1999)
54. E. Corredor et al., BMC Plant Biol. **9**, 45 (2009)
55. Z. Cifuentes, L. Custardoy, J.M. de la Fuente, C. Marquina, M.R. Ibarra, D. Rubiales, A. Perez-De-Luque, J. Nanobiotechnol. **8**, 26 (2010)
56. A. Di Pietro, M.P. Madrid, Z. Caracuel, J. Delgado-Jarana, M.I.G. Roncero, Mol. Plant Pathol. **4**, 315 (2003)
57. E.I. Boutati, E.J. Anaissie, Blood **90**, 999 (1997)
58. S.Z. Validov, F.D. Kamilova, B.J.J. Lugtenberg, Microb. Biotechnol. **4**, 82 (2011)
59. H.R. Rechenberg, J.A.H. Coaquira, C. Marquina, B. Garcia-Landa, M.R. Ibarra, A.M. Benito, W. Maser, E. Munoz, M.T. Martinez, J. Magn. Magn. Mater. **226**, 1930 (2001)
60. J.A.H. Coaquira, H.R. Rechenberg, C. Marquina, M.R. Ibarra, A.M. Benito, W. Maser, E. Munoz, M.T. Martinez, Hyperfine Interact. **134**, 103 (2001)
61. R. Fernández-Pacheco, Ph.D. Thesis, Universidad de Zaragoza, 2008
62. W. Kratschmer, L.D. Lamb, K. Fostiropoulos, D.R. Huffman, Nature **347**, 354 (1990)
63. A. Perez de Luque, M.D. Lozano, J.I. Cubero, P. Gonzalez-Melendi, M.C. Risueno, D. Rubiales, J. Exp. Bot. **57**, 931 (2006)
64. S. Martin-Ortigosa, K. Wang, Transgenic Res. **23**, 743 (2014)
65. M. Bottini, S. Bruckner, K. Nika, N. Bottini, S. Bellucci, A. Magrini, A. Bergamaschi, T. Mustelin, Toxicol. Lett. **160**, 121 (2006)
66. A. Pavel, M. Trifan, Bara, II, D.E. Creanga, C. Cotae, J. Magn. Magn. Mater. **201**, 443 (1999)
67. V. Cotae, L. Creanga, J. Magn. Magn. Mater. **289**, 459 (2005)
68. A. Pavel, D.E. Creanga, J. Magn. Magn. Mater. **289**, 469 (2005)
69. A.K.M. Ekramoddoullah, R.S. Hunt, Can. J. Plant Pathol.-Rev. Canadienne De Phytopathologie **24**, 408 (2002)
70. T. Eichert, A. Kurtz, U. Steiner, H.E. Goldbach, Physiol. Plant. **134**, 151 (2008)
71. A. Perez de Luque, J. Jorrin, J.I. Cubero, D. Rubiales, Weed Res. **45**, 379 (2005)
72. K.J. Oparka, S.S. Cruz, Annu. Rev. Plant Physiol. Plant Mol. Biol. **51**, 323 (2000)
73. E. Onelli, C. Prescianotto-Baschong, M. Caccianiga, A. Moscatelli, J. Exp. Bot. **59**, 3051 (2008)
74. G. Sarret et al., Plant Physiol. **141**, 1021 (2006)
75. L. De Matteis, L. Custardoy, R. Fernandez-Pacheco, C. Magen, J.M. de la Fuente, C. Marquina, M. Ricardo Ibarra, Chem. Mater. **24**, 451 (2012)
76. J.E. Puhalla, Canadian J. Botany-Revue Canadienne De Botanique **63**, 179 (1985)
77. E.A.M. Schoffelmeer, F.M. Klis, J.H. Sietsma, B.J.C. Cornelissen, Fungal Genet. Biol. **27**, 275 (1999)
78. R.L. Brandao, I.M. Castro, J.B. Passos, J.R. Nicoli, J.M. Thevelein, J. Gen. Microbiol. **138**, 1579 (1992)